Reconfigurable, Circularly Polarized and Scanning Antennas for Wireless Networks

Branka Jokanovic, *Member, IEEE*

Abstract—This paper presents some innovative antenna designs with enhanced performances for the next generation of wireless networks. High-gain printed microwave and millimeter wave antennas, both linearly and circularly polarized are discussed as well as reconfigurable circularly polarized antenna with switchable sense of polarization. Special attention has been devoted to the design of frequency scanning antennas based on matamaterial-inspired phase shifters. All presented antennas demonstrate considerable improvement of the efficiency, bandwidth of operation, axial ratio and frequency sensitivity. Also, they are very simple for manufacturing even at millimeter wave frequencies.

Index Terms — Circular antenna, scanning antenna, phase shifter.

I. INTRODUCTION

FIFTH generation of wireless access (5G) is expected to provide dramatically improved data rate, capacity, improved coverage and reduce latency. Anticipated performance gains are:1000 times higher mobile data volume per area, 10 times to 100 times higher number of connected devices, 5 times reduced end-to-end latency, 10 times longer battery life, etc. Such enormous improvement of the performances will not be possible without radical rethinking of the current radio access technology.

The fundamental limitation for increasing data rates in current mobile network is bandwidth due to limited spectrum. For example all current mobile networks operate in the microwave range, below 6 GHz where the spectrum is extremely congested. The bandwidth of around 600 MHz is currently available for mobile networks, divided among operators. Maximum possible increase of the bandwidth in that range in the best-case scenario is by factor of 2, that is far below the required spectrum for 5G. In contrast to that, there are great amounts of unutilized spectrum at millimeter wavelengths, above 30 GHz. This is why mm-wave is a serious candidate for 5G, with a potential to achieve huge data rates, both for radio access and wireless backhaul.

But the operation in millimeter frequency range has many challenges, however, most notably higher propagation losses. Due to less pronounced diffraction, and smaller penetration depths, the main problem for millimeter waves propagation is in the case of non-line-of-sight (NLoS) propagation. NLoS propagation can be maintained by multiple access points i.e. multiple antennas and backup links between transmitter and receiver, even if one link is blocked. It also requires rapid re-

routing protocol, which enables fast detection of blockages followed by fast hand off. As the antenna gain is higher in millimeter-wave range for the same physical size, the radiated beam is narrower, which calls for adaptive beamforming to deliver maximal RF energy to the user, while tracking his movement. On the other hand, narrow beams reduce the interference from other users.

In this paper we present an overview of the recent development of high-gain, scanning and reconfigurable antennas obtained in the Project TR 32024 . Innovative design of these antennas and their excellent performances, which in many aspects outperform the characteristics of existing solutions, make them an excellent candidate for the future 5G networks. Simple design and cost-effective fabrication are also important features in the case when a huge number of antennas are planned to be used in the future 5G network.

II. HIGH-GAIN PRINTED ANTENNA ARRAYS

High-gain printed antenna that are expected to play an important role in future wireless access, are still a major challenge for the engineers especially in the millimeter frequency range. Here we will discuss the microstrip patch and dipole antenna arrays, both with linear and circular polarization, as well as the antenna with printed primary radiator inserted into circular-parabolic reflector.

A. Patch Antenna Array at 17 GHz

We present a highly directive printed antenna array consisting of 420 identical patch antennas for FMCW radar applications [5]. The array exhibits 3 dB-beamwidths of 2° and 10° in H- and E-plane, respectively, side lobe suppression better than 20 dB and gain about 30 dBi in the frequency range 16.9 - 17.3 GHz. To obtain the 2^0-beamwidth in H-plane, it is necessary to have 42 radiating elements in a linear subarray. Unlike corporate feeding network which offers high bandwidth, we apply here a series feeding which is the best solution for minimizing losses in the array with a large number of elements. However, serial feeding is very sensitive to the frequency change due to the progressive phase change of the series fed elements. To avoid scanning of the main beam while changing the frequency within the 400 MHz band, it was necessary to split horizontal subarray into two separate halves [6], of the following 21 radiating elements. In this way it is achieved that the main lobe is always pointed in the broadside direction, regardless of frequency variations.

Feeding points of the subarray halves are not placed in their centers, but moved towards the center of the antenna, so that

Branka Jokanovic is with the Institute of Physics, University of Belgrade, 118 Pregrevica, 11080 Belgrade, Serbia (e-mail: brankaj@ ipb.ac.rs).
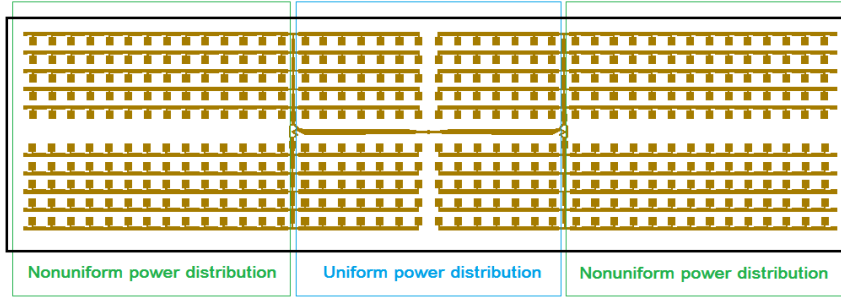
Fig. 1. Layout of the patch antenna array with marked regions with uniform and nonuniform power distribution. The overall antenna footprint is 31 λ_0 x 7.5 λ_0.
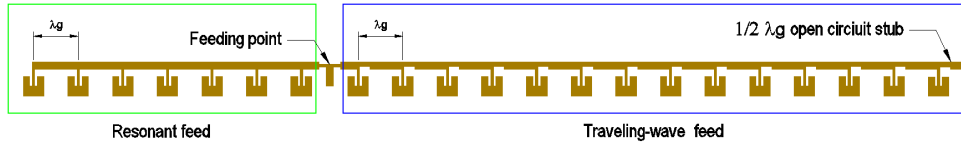
Fig. 2. The top right half of the H-plane subarray with two types of series feeding: resonant feed (left) and traveling-wave fee (right).
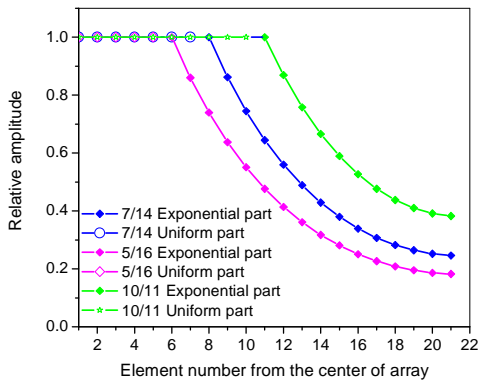
Fig 3. Different amplitude distributions along H-plane subarray.

(a)

(b)

Fig. 4. Simulated H-plane radiation patterns obtained using different amplitude distributions at: (a) 16.9 GHz and (b) 17.3 GHz.

there are 2 x 7 central patches between the feeding points with an uniform power distribution, while the rest of 2 x 14 patches are placed between the feeding points and the antenna edges and have an exponential distribution [7], as it is marked in the antenna layout (Fig. 1).

In order to increase the antenna efficiency we applied the optimized series feeding architecture in the H-plane with both resonant and traveling-wave feed as it is marked in Fig. 2. By varying the ratio of the number of elements with uniform and nonuniform distribution in the subarrays, the trade-off between the gain and 3-dB beamwidth on one side, and side-lobe suppression on the other side, can be adjusted. We have examine three different amplitude distributions shown in Fig. 3. which contain different number of uniformly fed (5, 7, 10) and exponentially fed (16, 14, 11) elements, respectively. Each distribution is denoted with the fraction N_u/N_{exp} which numerator N_u is equal to the number of elements with uniform distribution, while denominator N_{exp} indicates the number of elements having the exponential amplitude distribution. Simulated radiation patterns for different amplitude distributions are given in Fig. 4. It can be seen that the 10/11- distribution which

contains 10 elements with uniform distribution which contains 10 elements with uniform distribution exhibits very poor side lobe suppression of about 15 dB in the whole frequency band, while the 5/16-distribution has very good side lobe suppression of about 25 dB, but 3dB-beamwidth is 2.3^0 that is much wider than requested 2^0. As a compromise the 7/14-distribution is chosen for the design of H-plane subarray because it satisfies both requirements. The side lobe suppression is around 20 dB and 3-dB beamwidth is 2.1^0 in the whole frequency range.

B. Antenna Array with Cylindrical-Parabolic Reflector

Here a new type of printed antenna array with cylindrical-parabolic reflector [8] is discussed as an example of a very good solution for high-gain antennas at millimeter-wave frequencies. Antenna array operates at 60 GHz according to ECC Recommendation (09)01 – Use of the 57 – 64 GHz Frequency Band for Point-to-point fixed Wireless Systems [9]. This frequency range is characterized by high levels of oxygen absorption and rain attenuation that limits the range of communication systems. However it will allow a high level of frequency re-use and therefore makes it attractive for a variety of short-range communication applications. In addition to a very wide band point-to-point 60 GHz equipment with data rates comparable to that achieved by fiber optic technologies, there is interest in using that band for Radio Local Area Networks (RLANs) and for Wireless Metropolitan Area Networks (WMANs).

Printed antenna array which plays the role of the primary feed of cylindrical-parabolic reflector, consists of 16 pentagonal dipoles operating on the second resonance. Antenna array is integrated with the subreflector, feeding network and the transition from symmetrical microstrip to waveguide on the same dielectric substrate as it is shown in Fig. 5. Antenna array is placed on the focal line of the cylindrical-parabolic reflector as shown in Fig. 6.
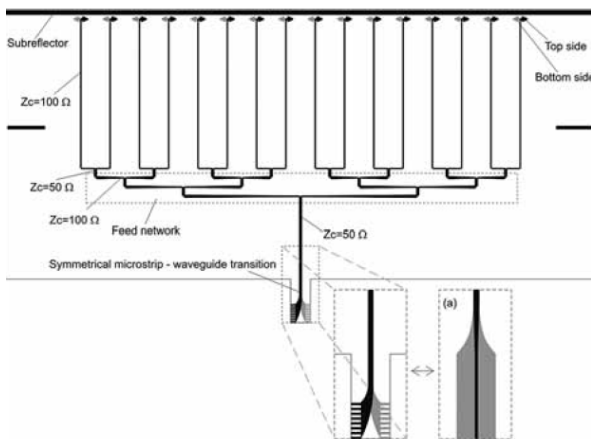
Fig. 5. Printed antenna array integrated with subreflector, feeding network and symmetrical microstrip –waveguide transition on the same dielectric substrate.

In this antenna a new type of a subreflector realized with a strip printed on both sides of the substrate along and ahead of the linear axial array is applied for the first time. The axis of the proposed printed subreflector and longitudinal axis of the array are spaced $\lambda/4$ apart. Such subreflector enables more compact design of the antenna with a smaller F/D ratio, i.e. smaller antenna depth. In this design the effect of aperture blocking which degrades the side lobes suppression (SLS) is practically avoided, which is the important advantage over conventional parabolic Cassegrain antennas with a subreflector. By use of such subreflector simulated gain is increased by 2 dB, SLS in H-plane is 3dB lower while it is 2 dB higher in E-plane than in the same case without a subreflector as can be seen from Figs. 7-8.
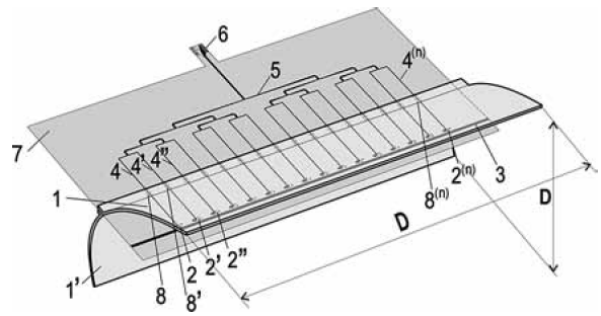
Fig. 6. Layout of the printed antenna array placed between two halves of the cylindrical-parabolic reflector: 1 and 1' - two halves of the parabolic reflector; 2–2$^{(n)}$ - printed pentagonal dipoles; 3 - subreflector; 4–4$^{(n)}$ - 100 Ω-lines of the feed network; 5 - feed network; 6 - transition from the symmetrical microstrip to a waveguide; 7 - dielectric substrate; 8–8$^{(n)}$ - holes in the cylindrical-parabolic reflector (n= number of dipoles in the array).
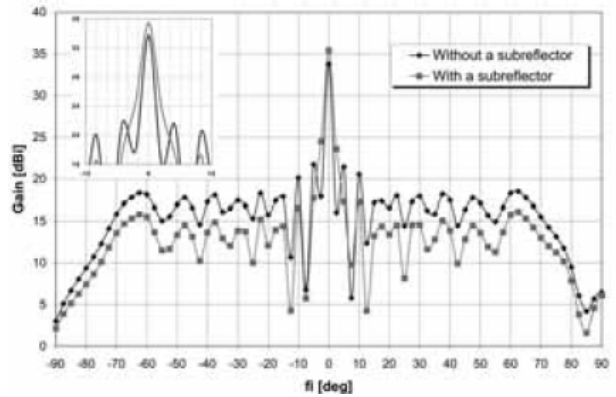
Fig. 7. Simulated H-plane radiation patterns of the antenna with and without a printed subreflector.
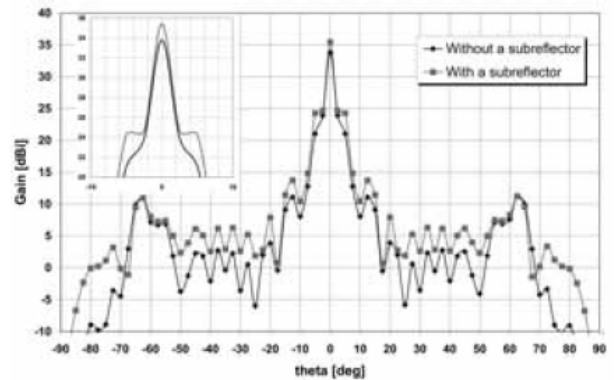
Fig. 8. Simulated E-plane radiation patterns of the antenna with and without a printed subreflector.

C. Printed Antenna Array with Circular Polarization

Circularly polarized antenna have several advantages over linearly polarized as well as greater flexibility in orientation of the transmitters and receivers and a greater immunity to multi-path interferences and fading [10], which makes them a key technology for various modern wireless systems.
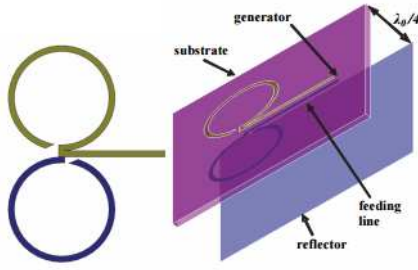
Fig. 9. Circularly polarized dipole antenna and reflector.
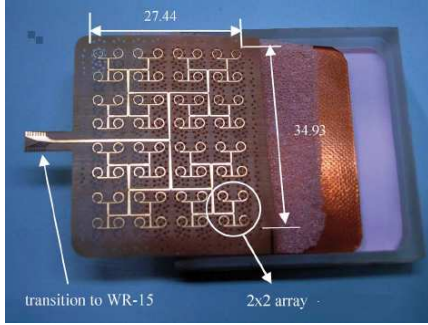
Fig. 10. Photograph of fabricated two-dimensional 8 x 8 antenna array at 60 GHz.
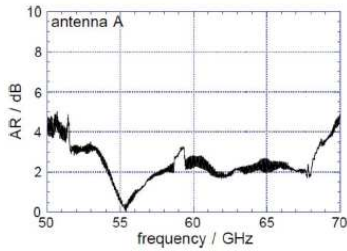
Fig. 11. Measured axial ratio (AR) of the antenna array.
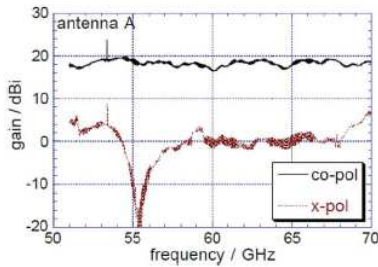
Fig. 12. Measured gain and X-polarization.

Two-dimensional 8 x 8 antenna array with open ring-dipoles [11] is one of the most interesting solutions for the printed high-gain circularly polarized antennas at millimeter-wave frequencies. The basic antenna dipole and reflector are shown in Fig. 9. In order to obtain better suppression of unwanted higher modes and surface waves, the antenna array is realized on a single perforated dielectric substrate along the corporate feeding network with impedance transformers as shown in Fig. 10. Because of its simplicity this design can be easily scaled to very high frequencies up to 110 GHz.

Antenna characteristics are measured in the frequency range 50-70 GHz and the results are shown in Figs. 11-13. It can be seen that measured axial ratio (AR) is bellow 3 dB within frequency range of 25 % around 60 GHz. Measured

gain is around 20 dBi and X-polarization attenuation is about 20 dB.
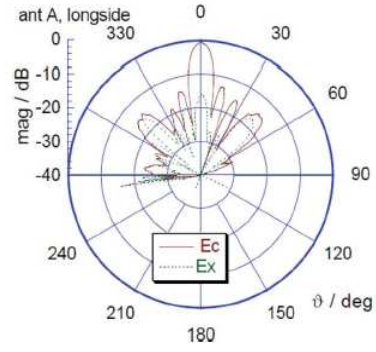
Fig. 13. Measured radiation pattern of the antenna at 61.5 GHz.

III. SCANNING ANTENNAS

Frequency-modulated continuous-wave (FMCW) radar in combination with frequency scanning antenna can provide low-cost solution to measuring target position distance and angle using a minimum of digital signal processing [12]. Commercial application of the direct imaging radar sensor depends mainly of the availability of cost-effective frequency scanning antennas.

Two types of printed frequency scanning antennas are presented: (a) the scanning antenna with metamaterial-based phase shifters [13]-[14] and (b) millimeter-wave holographic antenna [15]-[16].

A. Scanning antenna with metamaterial-based phase shifters

The proposed a compact frequency scanning antenna array consists of four linear subarrays with eight series-fed pentagonal dipoles specially optimized to exhibit a wide input impedance range from 120 to 1070 Ω. Two different phase shifters based on split-ring resonators are considered: (a) right-handed and (b) left-handed phase shifter as shown in Fig. 14. Right-handed phase shifter is chosen for the antenna design because of its simplicity and ability to scale to higher frequencies. Identical phase shifters are placed between dipoles along feeding line, and they are designed as a second-order bandpass filter with low insertion loss and very good matching. The layout of planar antenna array is shown in Fig. 15. Antenna exhibits an excellent characteristics: the scan sector of 55°, frequency sensitivity of 14.25°/100 MHz and low sidelobe levels of around −20 dB in the whole scanning frequency range as can be seen in Fig. 16.

B. Scanning Holographic Antenna

The operating principle of holographic antenna is based on optical holography as shown in Fig. 17. Antenna far field radiation pattern is formed by interference between the reference wave, which is in our case the surface-wave (SW) and hologram. Hologram consists of a series of periodic semi-circular, ellipsoidal or the straight metal strips.

To excite a propagating surface-wave mode on a dielectric slab, its permittivity should be high and the thickness should be larger than $\lambda_{ref}/10$ where λ_{ref} is the effective wavelength of the surface-wave mode.
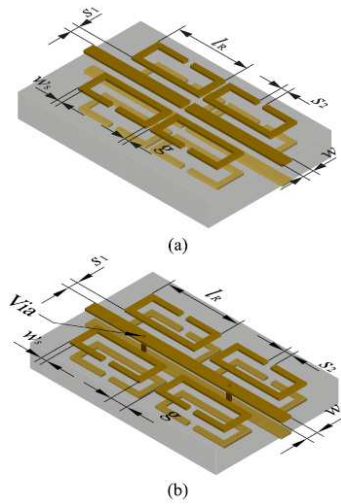
Fig. 14. The split-ring resonator-based phase shifters with relevant dimensions: (a) right-handed and (b) left-handed phase shifter.
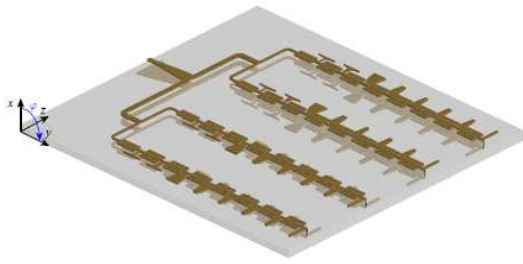
Fig. 15. Layout of the planar array antenna with 4×8 pentagonal dipoles.
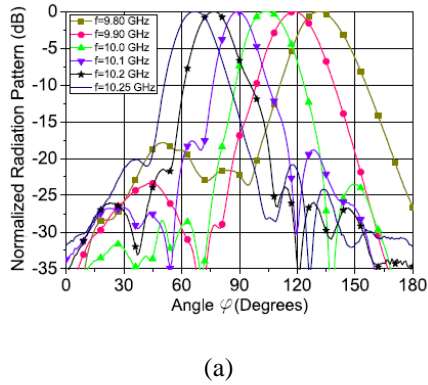
(a)
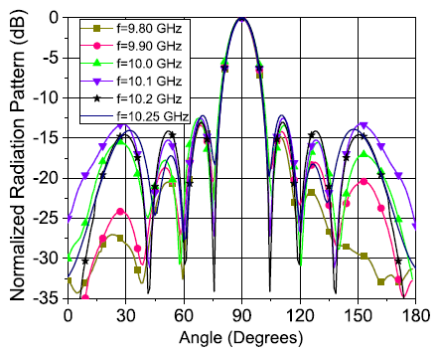
(b)

Fig. 16. Measured relative radiation pattern for the planar antenna array in: (a) H-plane and (b) E-plane.
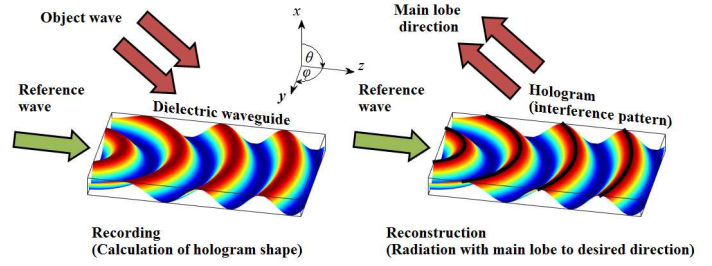
Fig. 17. Holographic principle for antenna technology: calculation of hologram shape and radiation with main lobe to desired direction.

Also, the angle range of the frequency-scanning beam-forming is increased if the holographic antenna uses thick substrates with a high permittivity. Holographic antenna is very promising solution for millimeter-wave frequencies due to its simplicity and easy integration with planar RF front-ends. It can provide a wide scanning range with optimized launcher. Simulated holographic antenna is shown in Fig. 18. It exhibits gain of 18.3 dBi, 3-dB-beamwidth of 7.4^0 while main beam is scanned for 1.4^0 from broadside direction.
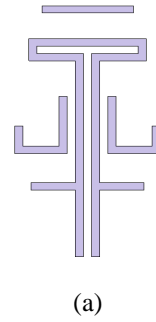
(a)
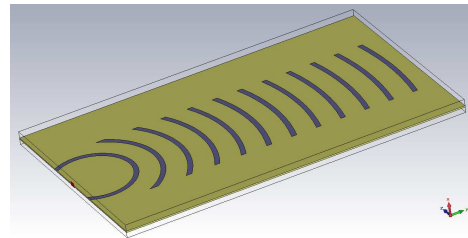
(b)

Fig. 18. Simulated holographic antenna: (a) uniplanar surface-wave launcher,
(b) hologram with overall dimensions 30 mm x 49 mm.
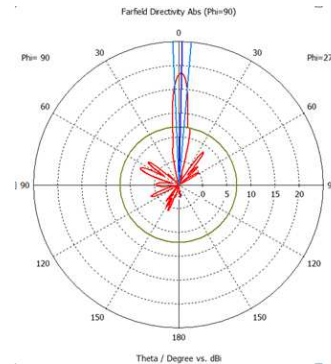
(a)
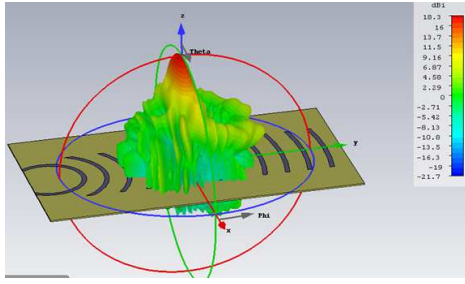
(b)

Fig. 19. Simulated radiation pattern at 60 GHz: (a) polar diagram, (b) 3D radiation pattern.

IV. RECONFIGURABLE ANTENNA

Very interesting solution for reconfigurable circularly polarized antenna with possibility of switching sense of circular polarization is shown in Fig. 20. Antenna consists of a pair of crossed dipoles fed by a symmetrical microstrip line and an identical additional inductive dipole on the opposite side of the substrate. Inductive dipoles are alternately connected to the capacitive dipole by means of PIN diodes, changing in that way the physical structure of the antenna, which results in switching the polarization sense between the left-hand (LHCP) to right-hand (RHCP). Radiation patterns in E- and H-panes for both polarizations at the central frequency of 6 GHz are presented in Fig. 21. Antenna has operational range of 7 % around 6 GHz with AR less than 3 dB.
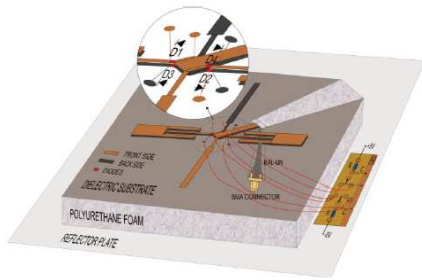
Fig. 20. Layout of the antenna structure above the reflector plane.
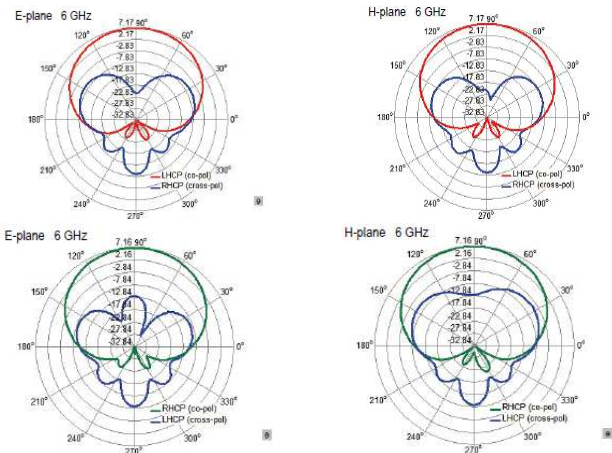
Fig. 21. Simulated radiation pattern in: E- and H-planes when LHCP is switched ON (above), and when RHCP is switched ON (down) respectively.

V. CONCLUSION

We have presented several advanced antenna designs achieved during the Project TR 32024, which are very applicable to the fifth generation of wireless access such as: the high-gain antennas, operating at millimeter wave band, frequency scanning antennas for the direct imaging radar sensors and the reconfigurable circularly polarized antenna with possibility of switching sense of circular polarization. All presented antennas can be considered the state-of-the-art in its field.

REFERENCES

[1] N. Boskovic, B. Jokanovic, F. Oliveri, D. Tarchi, "Highly Directive Patch Antenna Array for FMCW Radar at Ku Band," *Microwave Review*, vol. 21, no. 2 pp. 14-18, Dec. 2015.

[2] Huang, J, "Parallel-Series-Fed Microstrip Array with High Efficiency and Low Cross-Polarization", *Microwave and Optical Technology Letters*, Vol. 5, No. 5, pp. 230-233, May 1992.

[3] M. Slovic, B. Jokanovic, B. Kolundzija, "High Efficiency Patch Antenna for 24 GHz Anticollision Radar", in *Proc. 7th Int. Conf. Telecommun. Modern Satellite, Cable and Broadcasting Services,* Nis, Serbia, Sept. 28-30, 2005, pp. 20-23.

[4] A. Nesic and I. Radnovic, "60 GHz Range High Gain Printed Antenna Array with a Cylindrical-Parabolic Reflector", *Frequenz, Journal of RF Engineering and Telecommunications*, no. 64 (2010), 3-4, pp. 48-51.

[5] ECC Recommendation (09)01 – Use of the 57 –64 GHz Frequency Band for Point-to-point fixed Wireless Systems, Electronic Communications Committee (ECC) "Spectrum Engineering" (SE)), pp.1 –2

[6] Steven (Schichang) Gao, Qi Luo, Fuguo Zhu, *Circularly Polarized Antennas*.: John Wiley & Sons Ltd., 2014.

[7] A. Nesic, D. Nesic, "Printed Planar 8x8 Array Antenna with Circular Polarization for Millimeter-Wave Application", *IEEE Antenna Wireless Propagation Letters*, vol. 11, pp. 744-747, 2012.

[8] W. Mayer, M. Wetzel, and W. Menzel, "A novel direct-imaging radar sensor with frequency scanned antenna," *IEEE MTT-S Int. Microw. Symp. Dig.*, vol. 3. Jun. 2003, pp. 1941–1944.

[9] N. Boskovic, B. Jokanovic, M. Radovanovic, "Printed Frequency Scanning Antenna Arrays With Enhanced Frequency Sensitivity and Sidelobe Suppression", *Trans. Antennas Propag.*, vol. 65, no. 4, pp.1757-1764, Apr. 2017.

[10] N. Boskovic, B. Jokanovic, and A. Nesic, "Frequency scanning antenna array with enhanced side lobe suppression," in *Proc. 8th Int. Congr. Adv. Electromagn. Mater. Microw. Opt.*, Aug. 2014, pp. 67-69.

[11] C. Rusch, J. Schäfer, H. Gulan, P. Pahl, and T. Zwick, "Holographic mmW-Antennas With TE_0 and TM_0 Surface Wave Launchers for Frequency-Scanning FMCW-Radars," *Trans. Antennas Propag.* vol. 63, no. 4, pp. 1603-1612, Apr. 2015.

[12] S. Podilchak, , A. P. Freundorfer, and Y. M. M. Antar, "Surface-Wave Launchers for Beam Steering and Application to Planar Leaky-Wave Antennas," *Trans. Antennas Propag.,* vol. 57, no. 2, pp.355-363, Feb. 2009.

[13] I. Radnovic and A. Nesic " Printed Crossed Dipoles Antenna with Switchable Sense of Circular Polarization, *Microwave Review*, vol. 22, no. 2, pp. 27-30. Dec. 2016.

[14] Vojislav Milosevic, Branka Jokanovic, Olga Boric-Lubecke, Victor M. Lubecke, "Key Microwave and Millimeter Wave Technologies for 5G Radio," in *Powering the Internet of Things with 5G Networks*, V. Mohanan, R. Budiatru, I. Aldmour, Eds. IGI Global, to be published.

[15] O. Boric-Lubecke, V. M. Lubecke, B. Jokanovic, A. Singh, E. Shahhaidar and B. Padasdao, "Microwave and wearable technologies for 5G," *Telecommunication in Modern Satellite, Cable and Broadcasting Services (TELSIKS), 2015 12th International Conference on*, Nis, 2015, pp. 183-188.